Cement & Concrete Composites 37 (2013) 61–67

Contents lists available at SciVerse ScienceDirect

Cement & Concrete Composites

journal homepage: www.elsevier.com/locate/cemconcomp

Primary particle size and agglomerate size effects of amorphous silica in ultra-high performance concrete

Tina Oertel [a,b,*], Frank Hutter [a], Ricarda Tänzer [c], Uta Helbig [a], Gerhard Sextl [a,d]

[a] Fraunhofer-Institute for Silicate Research ISC, Neunerplatz 2, 97082 Würzburg, Germany
[b] Inorganic Chemistry I, University Bayreuth, Universitätsstr. 30, 95440 Bayreuth, Germany
[c] Building Materials and Construction Chemistry, Technical University Berlin, Gustav-Meyer-Allee 25, 13355 Berlin, Germany
[d] Technology of Advanced Materials, Julius Maximilians University, Röntgenring 11, 97082 Würzburg, Germany

ARTICLE INFO

Article history:
Received 8 October 2012
Received in revised form 3 December 2012
Accepted 6 December 2012
Available online 19 December 2012

Keywords:
Silica fume
Ultra-high performance concrete
Amorphous silica
Stoeber particles
Particle size distribution
Compressive strength

ABSTRACT

Silica fume is widely used in ultra-high performance concrete (UHPC). However, it is a by-product in the industrial silicon production and therefore far from an optimized additive. Silica fume improves the compressive strength, but its detailed reaction mechanisms in concretes with low water/cement ratios are not yet fully understood. This study focuses on the influence of primary particle sizes and sizes of agglomerates of different amorphous silicas in UHPC. As a reference system, wet-chemically synthesized silica was used with very high purity, defined particle sizes, narrow primary particle size distributions and controllable agglomerate sizes. The obtained data were compared to silica fume. The results indicate that non-agglomerated silica particles produce the highest strength after 7 d, but a clear dependence on primary particle sizes, as suggested by calculations of packing density, was not confirmed. UHPC may be improved by incorporating an ameliorated dispersion of silica e.g. through commercial silica sols.

1. Introduction

In recent years, ultra-high performance concrete (UHPC) has generated considerable interest due to its high compressive strength, dense structure and low capillary porosity [1]. The next generation of infrastructure will very likely necessitate fiber-reinforced UHPCs to fulfill the demands of flexural strength, toughness and durability [2].

Since the 1990s, the particle packing density has become a central aspect in the formulation of UHPCs [2]. Geisenhanslücke [3] presents an excellent summary of the particle packing theories and their further development to suit UHPC formulations. Submicrometer particles are the key ingredient because they fill pores between larger particles of cement, sand and other fillers. Commonly, undensified silica fume is used for this purpose [4]. Due to the low water/cement (w/c) ratios (<0.25 by mass) in UHPC systems, pozzolanic reaction of the silica with portlandite from clinker hydration to form C–S–H-phases is limited and the filler effect seems to be predominant.

Although many investigations exist on the function of silica fume in concrete, it is still of interest how silica fume or other forms of silica could be improved in terms of purity, particle size and particle size distribution to exhibit even better results. The optimization of silica addition may lead to further improvements of UHPC. But, as a by-product of an industrial production process silica fume is far from an optimized concrete additive [5]. It lacks in purity and a controllability of the particle size and the particle size distribution [6,7]. How these characteristics influence the performance of UHPC is still unclear.

To answer this question, we prepared UHPC with wet-chemically synthesized silica (Stoeber particles [8]) as a reference system. These spherical particles have a high chemical purity (SiO_2 of 99.97 wt.%), a definable particle size and a narrow particle size distribution. Furthermore, agglomeration of these particles can be avoided. Particle size ranges from 72 nm to 720 nm to cover the primary particle size distribution of the silica fume used.

We investigated the effects of these particle characteristics on the calculated particle packing densities, the microstructure and the compressive strength of UHPC. The nearly monomodal size distribution of Stoeber particles allows one to correlate particle sizes with calculated particle packing densities and compressive strengths. Also different states of dispersion are considered by adding silica dispersed to primary particle sizes (suspension) or as agglomerated particles (powder).

* Corresponding author at: Fraunhofer-Institute for Silicate Research ISC, Neunerplatz 2, 97082 Würzburg, Germany. Tel.: +49 (0) 3643/4100 511; fax: +49 (0) 3643/4100 399.
E-mail address: tina.oertel@isc.fraunhofer.de (T. Oertel).

0958-9465/$ - see front matter © 2012 Elsevier Ltd. All rights reserved.
http://dx.doi.org/10.1016/j.cemconcomp.2012.12.005

2. Experimental procedures

2.1. Synthesis of Stoeber suspensions and powders

Stoeber suspensions were synthesized by hydrolysis and condensation of tetraethyl orthosilicate (TEOS) to amorphous silica particles in an ethanolic solution with ammonia (NH_3) catalysis [8].

$$Si(OC_2H_5)_4 + 2H_2O \rightarrow SiO_2 + 4C_2H_5OH$$

The particle size (e.g. 72, 143, 242, 433 and 720 nm) is adjustable by the relative concentrations of precursors (TEOS, H_2O) and catalyst (NH_3).

After synthesis, ethanol was stepwise exchanged with water by rotary evaporation. The further treatment was twofold. The aqueous Stoeber suspension was concentrated to a solids content of 50 wt.% by further rotary evaporation. During the whole process, the temperature was maintained below 40 °C. Otherwise, powders of Stoeber particles were obtained by spray drying (Buechi spray dryer B-290, inlet temperature 220 °C, outlet temperature 105 °C) of aqueous Stoeber suspensions (solids content approx. 1 wt.%) [9].

2.2. Components of UHPC mortars

UHPC mortars were prepared from Portland cement type CEM I 52.5R HS/NA (Holcim Sulfo 5, Holcim AG, Germany) with high initial strength (R), high sulfate resistance (HS) and low alkali content (NA). An analysis of the clinker phases was provided by the supplier (in wt.%: C_3S = 64.6, C_2S = 12.8, C_3A = 0.2 and C_4AF = 16.6). The aggregates used were quartz powder and quartz sand (W12: 0.3–110 μm and F32: 0.125–0.5 mm, Quarzwerke Frechen, Germany). Polycarboxylate ether (ViscoCrete®-2810, Sika GmbH, Germany) was used as superplasticizer. Its water content of 60 wt.% was considered in the calculation of the w/c ratio (0.23).

Silica addition was either Stoeber particles (Section 2.1) or silica fume (Sika® Silicoll P, Sika GmbH, Germany) which was an "as produced" fume and therefore never exposed to a densification process.

2.3. UHPC mortar and sample preparation

The applied UHPC formulation (Table 1) is based on M3Q. M3Q was developed at the University of Kassel and its composition was optimized for dense particle packing (see Sections 2.5 and 3.2) [10]. Samples without any silica were prepared besides samples with Stoeber particles or silica fume.

Mortars were mixed in two different procedures:

(a) Silica powders were premixed with cement, quartz sand and quartz powder for 30 min in a tumbling mixer. Superplasticizer was dissolved in water. This solution was added to the powder blend and mixed with a handheld kitchen mixer for 4.5 min (procedure: 3 min mixing, 1 min break, 1.5 min mixing).
(b) For preparations with silica suspensions, the superplasticizer was first mixed with the cement in a grinding dish. This pretreated cement was mixed with quartz sand and quartz powder in a tumbling mixer (30 min). Then, the silica suspension was added to the tumbled powder blend and mixed with the handheld mixer for 4.5 min. The solids content of the silica suspension (50 wt.%) was adjusted to represent the appropriate amount to fully replace water and silica in the UHPC formulation. This mixing procedure was necessary because attempting to dissolve the superplasticizer in the silica suspension leads to gelation or precipitation.

Table 1
UHPC formulation with w/c = 0.23, formulation based on M3Q [10].

Material	Density (g/cm^3)	Composition (kg/m^3)
Water	1.0	175.0
Portland cement	3.0	825.0
Stoeber particles or silica fume	2.2	175.0
Quartz powder	2.7	200.0
Quartz sand	2.7	975.0
Superplasticizer	1.1	27.5

For each set of Stoeber particles (mean primary particle sizes of 72, 143, 242, 433 or 720 nm), two mortars were prepared: one with the corresponding suspension (procedure b) and one with the spray dried powder (procedure a). Also silica fume was added either as a powder as received from the supplier or as 50 wt.% aqueous suspension from preparation with an ultrasonic wand (Branson Sonifier 450).

5–10 samples (die: 2 × 2 × 2 cm^3) were cast from each mortar and stored for 2 d in their molds and for 5 d in water at 20 °C. The restricted number of samples and the small specimen size result from the limited laboratory batch size of Stoeber particles.

2.4. Characterization methods and test procedures

Characterization of silica was done by X-ray diffraction (Philips PW 1710) and X-ray fluorescence spectroscopy (PANalytical Axios-Advanced).

Particle sizes of silica (⩽approx. 800 nm) were measured by dynamic light scattering (DLS; Malvern Zetasizer Nano-ZS ZEN3600, polystyrene cuvettes) in diluted suspensions (0.3 wt.%). These suspensions were obtained by diluting the 50 wt.% silica suspensions (Stoeber particles suspension from Section 2.1 and silica fume suspension from Section 2.3) to avoid multiple scattering. Larger particles (e. g. agglomerates) were measured by Fraunhofer diffraction (FD; Malvern Mastersizer S, 0.005–900 μm lens) in diluted suspensions (approx. 0.05 wt.%).

The particle sizes of cement and quartz powder were measured with a laser granulometer (Beckman-Coulter LS 230). 0.05 g cement or 0.25 g quartz powder were dispersed in 15 ml water with $Na_4P_2O_7$ (c = 1.5 g/l), which acts as a dispersion additive and hydration inhibitor, and ultrasonic treatment (Branson Sonifier 250). Comparative measurements in isopropyl alcohol (data not shown) confirmed that $Na_4P_2O_7$ prevented the dissolution and flocculation of cement effectively throughout the measurement (2 min).

The particle size of quartz sand was measured with the sieve analysis (mesh size: 1000, 800, 500, 200, 125, 90, 63, 40 and 32 μm).

Silica particles in the microstructure of UHPC samples (7 d after mortar preparation) were observed by scanning electron microscopy (SEM; Carl Zeiss Supra 25) on argon ion beam polished cross-sections of an unbroken UHPC sample (cross section polisher CSP; JEOL SM-09010). This preparation method alters the material to a minimum extent and allows the observation of water sensitive materials [11].

The intrudable pore volume [12] of hardened samples was determined by mercury intrusion porosimetry (Quantachrome Poremaster 60 GT). For this analysis, broken samples from the compressive strength testing were dried via vacuum drying at 20 °C until a constant weight was reached.

The compressive strength was measured 7 d after sample preparation (ToniZEM device).

2.5. Calculation of particle packing density

Calculations of the particle packing density were performed with the program WinCem (spreadsheet based) which was developed by the research group of Professor Schmidt from the Univer-

sity of Kassel [1]. The program is based on the computational algorithms of Schwanda to determine the void content of grain mixtures [13] and was improved for fine grained concretes by Reschke [14,15] and by Geisenhansluecke [3]. The particle packing density is calculated by combining the measured particle size distributions of all solid mortar components until the void content is minimized. Thereby the composition of a mortar with an optimized particle packing density is received. Moreover, the program can be used to calculate variations of particle packing densities by substituting a component.

3. Results and discussion

3.1. Characterization of silica

3.1.1. Chemical composition

The X-ray diffraction patterns (Fig. 1) are typical for amorphous silica showing a broad peak for a *d*-value of approx. 4 Å. For silica fume, additional weak peaks appear which correspond to SiC. This chemical compound results from the production process in the electric arc furnace and was also observed by others [16]. Correspondingly, silica fume has a lower purity than Stoeber particles (Table 2).

3.1.2. Primary particle size and agglomerate size

Silica fume and Stoeber particles consist of spherical primary particles (Fig. 2a and b). During spray drying (Section 2.1), agglomerates of Stoeber particles are formed (Fig. 3).

DLS measurements on ultrasonically treated diluted aqueous suspensions (Fig. 4) confirm the narrower particle size distributions for Stoeber particles in comparison to silica fume. Herein, silica fume covers the particle size range of Stoeber particles with d_{50} = 143, 242, 433, 720 nm and its mean particle size (d_{50} = 283 nm) is near to those Stoeber particles with d_{50} = 242 nm. Particle size distributions from Fig. 4 are used for subsequent particle packing density calculations (Section 3.2).

Agglomerates of Stoeber particles from spray drying have sizes of d_{50} = 3.5–5.0 μm which are independent from the primary Stoeber particle size (FD measurements in Fig. 5). Analogously measured silica fume has a broader size distribution (d_{50} = 17 μm) than spray dried Stoeber particles.

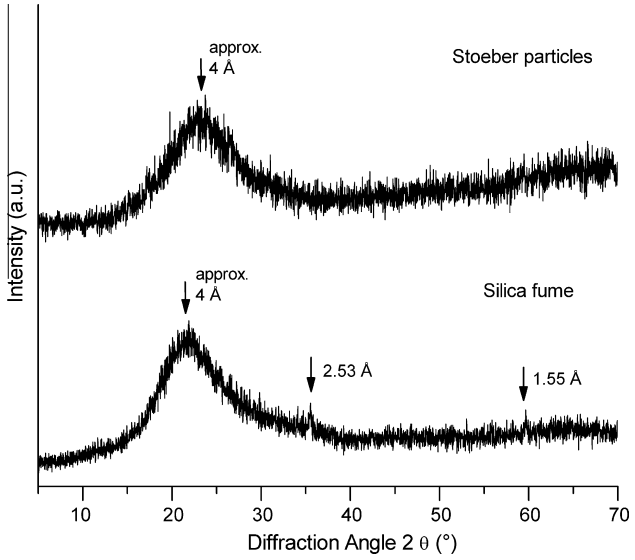

Fig. 1. X-ray diffraction patterns of silica. The broad peak at approx. d = 4 Å is the amorphous hump. Two weak reflexes in silica fume correspond to SiC.

Table 2
Analytical composition of silica extracted from X-ray fluorescence spectroscopy.

Content (wt.%)	Stoeber particles[a]	Silica fume
SiO_2	99.970	98.580
CaO	–	0.241
Al_2O_3	0.017	0.142
Fe_2O_3	0.005	0.031
SO_3	0.002	0.141
K_2O	–	0.533
Na_2O	–	0.093
MgO	–	0.162
Cl	–	0.011

[a] 242 nm particles serving as an example.

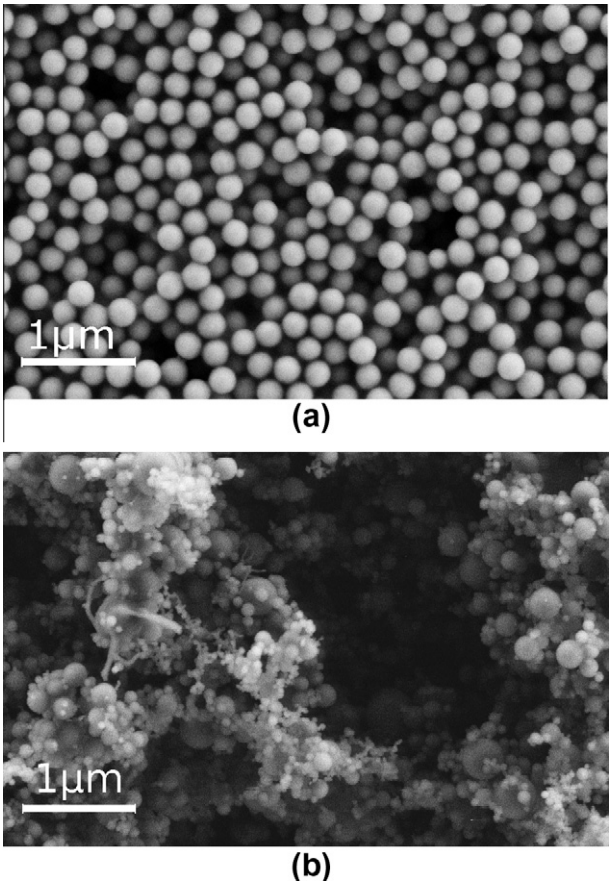

Fig. 2. SEM image: (a) 242 nm sized Stoeber particles, and (b) silica fume.

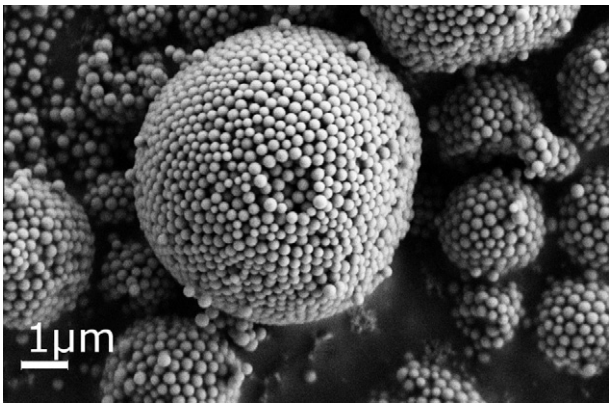

Fig. 3. SEM image of spray dried 242 nm sized Stoeber particles powders.

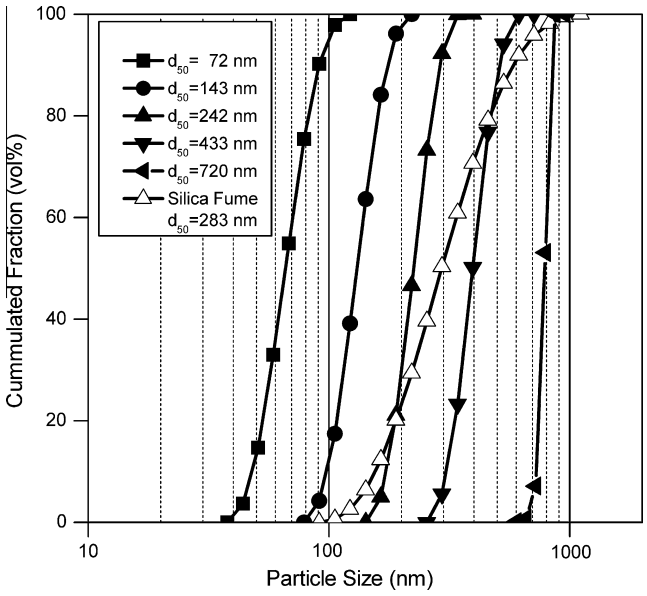

Fig. 4. Particle size distribution and mean primary particle size (d_{50}) of Stoeber particles and silica fume (DLS, 0.3 wt.% suspensions, average of three measurements). Data are used in particle packing density calculations.

The results from the Stoeber suspensions indicate that the Stoeber particles are dispersed to their primary particle sizes in the diluted suspensions which have been measured in DLS. There is a good possibility that the dispersion state is similar for undiluted Stoeber suspensions which are used in the UHPC formulations. Spray drying leads to agglomeration due to the formation of Si–O–Si bonds between primary particles. These agglomerates do not deagglomerate in water as is shown by the measured agglomerate sizes in FD.

To evaluate the received values for silica fume one can use the terminations 'clusters' and 'agglomerates' as they were given by Diamond and Sahu [7]. During the formation of silica fume at high temperature (>1000 °C) in the electric arc furnace, primary particles (spheres, e.g. seen in Fig. 2b) condense and are bound immediately to clusters of several spheres by sintered junctions throughout Si–O–Si bonds. Agglomerates of clusters form either when the material cools and is stored in the silo (undensified silica fume as used in this study) or in the air densification process (see e.g. [7]) to produce densified silica fume.

The particles detected in DLS have to be considered as clusters into which silica fume can be dispersed by using intensive ultrasonic treatment of an aqueous suspension (see Section 2.3). This finding corresponds to explanations of Diamond and Sahu [7]. There is a good possibility that the measured cluster size is similar to the clusters in the 50 wt.% suspension used for mortar preparation. Agglomerates (as measured in FD) will possibly exist in the mortar when silica fume is used as a powder. Despite an undensified silica fume being used, difficulties of dispersion are quite analogous to densified products [7,17].

In conclusion, it is possible to disperse silicas to their primary particle sizes (Stoeber particles) or clusters (silica fume) either when the particles were synthesized as a dispersion and never dried to a powder (Stoeber suspension) or when the silica powder is dispersed ultrasonically in high dilution (silica fume). Otherwise silica particles are compounded to agglomerates which are presumably not dispersible in the preparation procedure of a mortar. Overall, the results indicate that silica particles from Stoeber suspensions should provide the highest dispersion state when mixed into concrete.

3.2. Particle packing density

The calculation of the particle packing density is based on the UHPC formulation (Table 1) and the particle size distributions of silicas (Fig. 4) as well as of cement, quartz sand and quartz powder (Fig. 6). The results for the various silica components are given in Fig. 7. Herein, the particle packing density increases with decreasing mean particle sizes which is similar to the findings of Reschke [14]. For silica fume, the particle packing density is slightly lower than for the 242 nm Stoeber particles. The particle density reaches a maximum value of 0.834 for the 143 nm Stoeber particles. Smaller particles (72 nm) yield no higher values. The UHPC formulation without any silica particles shows the lowest particle packing density.

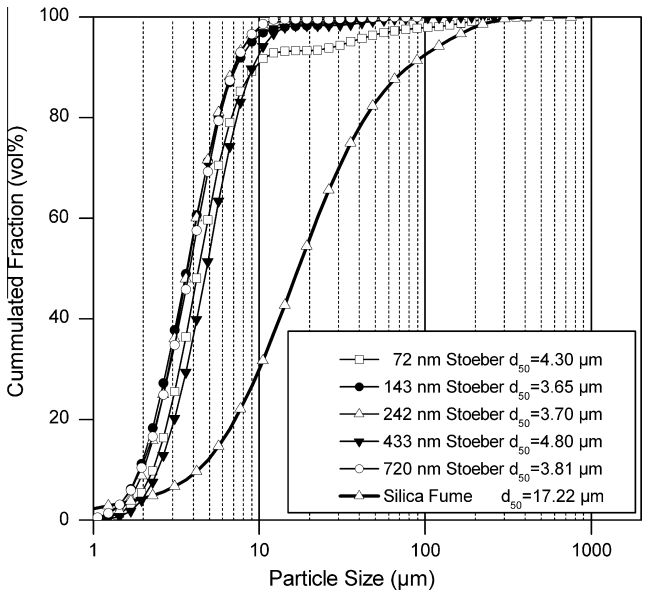

Fig. 5. Particle size distribution and mean particle size (d_{50}) of aqueous suspensions of spray dried Stoeber particle powders and silica fume (FD, 0.05 wt.% suspensions, average of four measurements).

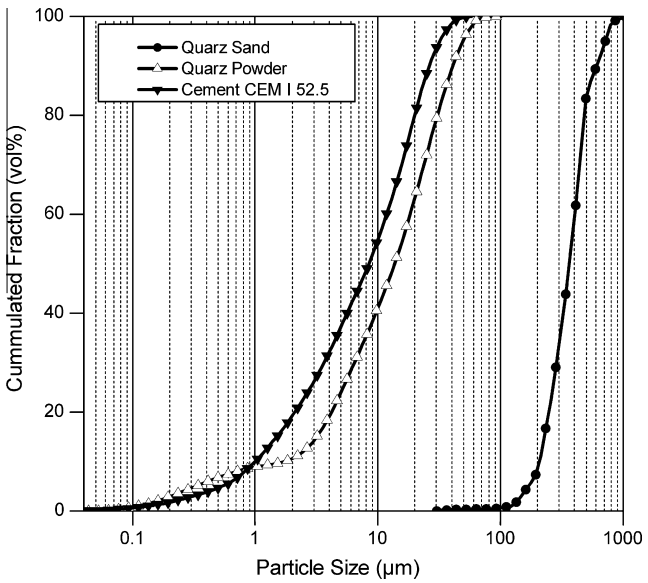

Fig. 6. Particle size distribution of quartz sand (sieve analysis), cement and quartz powder (laser granulometry). Data are used in particle packing density calculation.

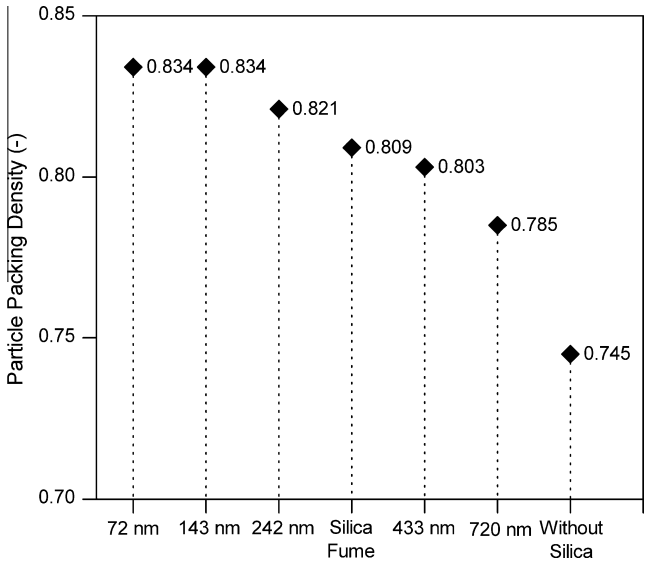

Fig. 7. Calculated particle packing density of UHPC with Stoeber particles (d_{50} from Fig. 4) and silica fume. The data show that the particle packing density increases with decreasing mean particle diameter.

One might expect that a silica fume with its broad particle size distribution (see Section 3.1.2) should result in a larger particle packing density because smaller particles can fill voids which are created by larger particles. However, the calculated particle packing density shows that a higher density can be reached with monomodal particles smaller than the average particle size of silica fume (d_{50} < 283 nm). This effect might result either from a beneficial effect of monomodal particles in filling voids of the overall composition or from their overall smaller size. The calculated particle packing densities result from the sizes of Stoeber primary particles and the cluster sizes of silica fume.

3.3. Characterization of hardened UHPC samples

3.3.1. Microstructure

Fig. 8 shows a representative image of the UHPC mortar microstructure 7 d after sample preparation at low magnification. Quartz grains (dark grey), cement grains (white) and the C–S–H/silica matrix (light grey) can be identified easily. The cracks result from the drying before sample preparation. At higher magnification, the amorphous silica particles are depicted amongst the C–S–H phases in the C–S–H/silica matrix (Fig. 9a–d). The imaged microstructures are derived from mortars with silica fume powder or 242 nm Stoeber particles applied as spray dried powder or suspension. For comparison, one sample is shown without any silica. Independent from the type of silica, the characteristics are very similar (Fig. 9a–c). Assemblages of silica particles (Stoeber and silica fume) are confined in a very dense matrix of C–S–H phases. The matrix of the sample without silica (Fig. 9d) looks more porous.

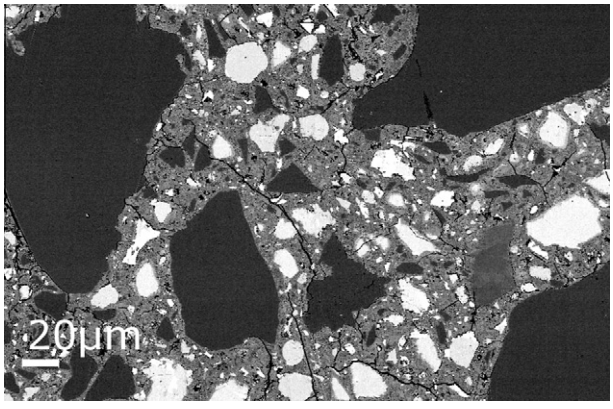

Fig. 8. SEM image of CSP prepared UHPC (7 d of hydration). The representative image of the microstructure shows quartz grains (dark grey), cement grains (white) and the C–S–H/silica matrix (light grey).

More quantifiable results for the porosities may be obtained from mercury intrusion. Samples without silica have a porosity of 11.3 vol.% which is higher than for samples with silica fume (7.8 vol.%). These porosities lie in the range of high-strength concretes (8.0–12.0 vol.%) [4]. With the calculated densities (Fig. 7), a free volume in the unreacted mixture of solid components is given (25.5% for mortars without silica and 19.1% for mortars with silica fume). These calculated free volumes and the measured porosities seem to be proportional. In conclusion, silica additions contribute to a more pronounced densification of hardened concrete. This finding corresponds to former observations [18].

3.3.2. Correlation of compressive strength, silica particle size and calculated particle packing density

Fig. 10 presents values of compressive strength for the UHPC samples (7 d after sample preparation). For 72 nm Stoeber particles (and even smaller silicas, not performed in this study), a castable mortar could be obtained only at an increased w/c ratio (0.30) due to the tremendously increased water demand for wetting additional silica surfaces [19]. The mortars with 143 nm Stoeber particles were the most viscous for the same reason. For all other silica, the mortars could be easily mixed to castable fluids despite their differing characteristics and differing procedures of silica application (powder or suspension). In this study it was not possible to verify this qualitative information with a slump test, due to the limited amounts of Stoeber particles available.

Samples without silica have the lowest strength. For the other mortars, only one tendency can be seen clearly due to the reasonable overlap of data standard deviations. The additions of the silica component as a powder result in lower strengths than the additions as suspensions.

Whether there is a reasonable dependence of compressive strength on size characteristics of the used silica component, may be judged by considering the linear correlation (Fig. 11) between the mean values of compressive strength (Fig. 10) and the calculated particle packing densities (Fig. 7). Although the particle packing density provides information on the "unhydrated state" of the components, its influence on the compressive strength is still noticeable when primary particles or clusters of amorphous silica were incorporated as a suspension into the mortar (Pearson correlation coefficient [20] $r = 0.85$). The correlation is considerably lower ($r = 0.51$) by application of silica powders. Assuming that strength is only a function of packing density, this result may be interpreted as implying that no mortar mixing procedure could completely disperse silica to the particle size distributions on which the packing density calculations were based. It is most likely that silica agglomerates of varying size and differing dispersability have a substantial influence on the achievable packing density and its effects on compressive strength.

As one may conclude from these findings, it is necessary to introduce particles as least agglomerated as possible to obtain the highest strength in UHPC. Commercial silicas provide such particles which are dispersed to their primary particle sizes (e.g. silica sols from ion exchange processes).

The impurity of silica fume (SiC) seems to have no negative influence on the compressive strength. It is shown that the silica fume suspension has a similar compressive strength to a Stoeber suspension with a comparable mean particle size.

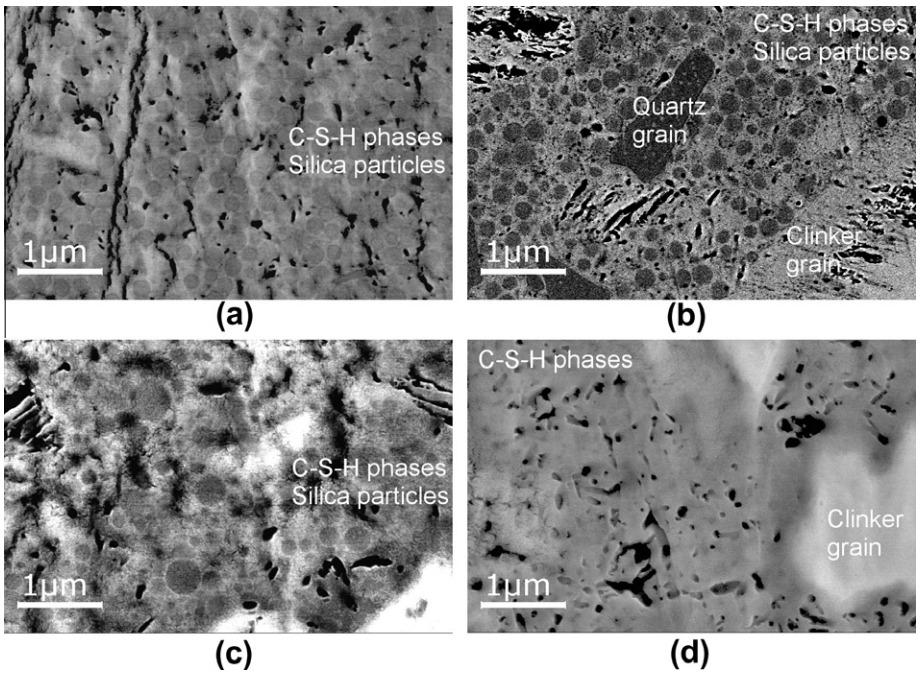

Fig. 9. SEM image of CSP prepared UHPC samples with different silica (7 d of hydration): (a) 242 nm sized Stoeber suspension, (b) spray dried 242 nm sized Stoeber powders, (c) silica fume powder, and (d) without silica. Assemblages of silica particles (Stoeber and silica fume) can be found confined in a very dense matrix of C–S–H phases. The matrix of C–S–H phases is more porous for UHPC without silica.

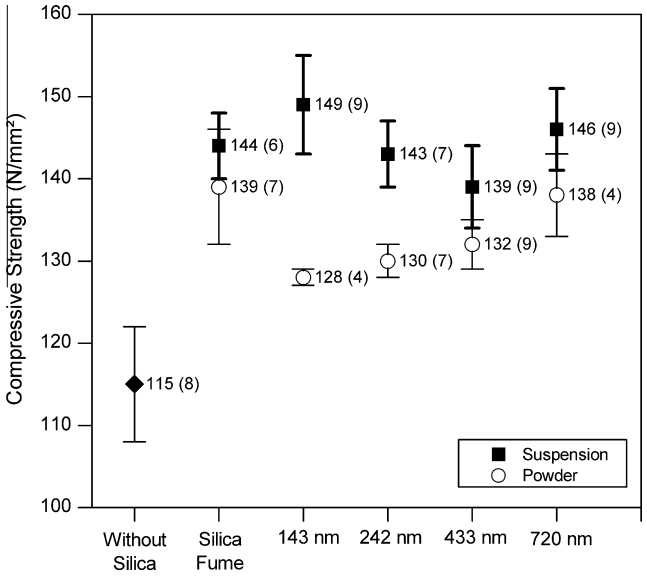

Fig. 10. Values for compressive strength (mean value and standard deviation, amount of samples is given in parenthesis) of UHPC at 7 d after sample preparation for Stoeber particles (d_{50} from Fig. 4) and silica fume. The data show that UHPC with silica suspensions has a higher strength than with silica powders.

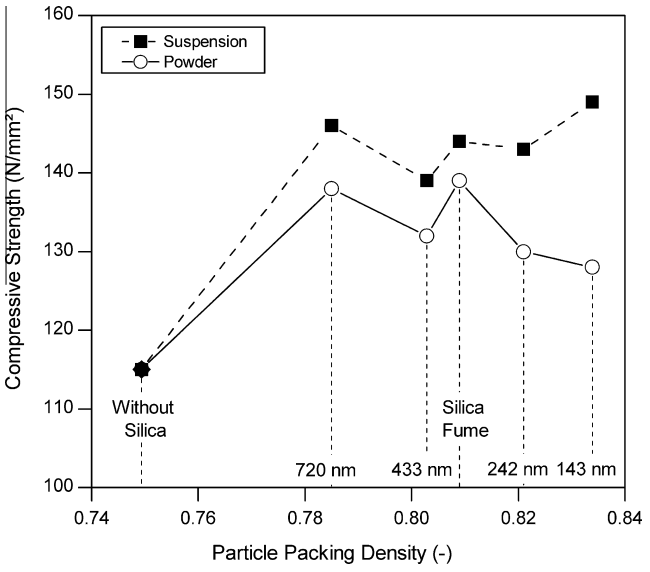

Fig. 11. Correlation of particle packing density (Fig. 7) and mean compressive strength (Fig. 9) of UHPC at 7 d after sample preparation for Stoeber particles (d_{50} from Fig. 4) and silica fume. The correlation is reasonable for silica suspensions (Pearson correlation coefficient $r = 0.85$) and low for silica powders ($r = 0.51$).

4. Conclusions

A commonly used silica fume was compared to wet-chemically synthesized silica (Stoeber particles of high purity, with defined primary particle sizes, narrow particle size distribution and in different agglomeration states) by application in an UHPC system.

The nearer the dispersion of the silica comes to primary particle sizes, the higher is the compressive strength (at least for 7 d after mortar mixing). Therefore, it is clear that the dispersion of silica into primary particle sizes or the smallest agglomerates possible is mandatory for further improvement of the compressive strength. This finding is consistent with others, e.g. [21]. Ideal silica fume dispersion by a common mortar mixing procedure might be impossible, but the dispersion of silica fume in water using ultrasound leads to at least some improvements [7]. Furthermore, commercial silicas should lead to higher strength if they provide particles dispersed to their primary particle sizes (e.g. silica sols from ion exchange processes).

The impurity of silica fume (SiC) seems to have no negative influence on the compressive strength.

With respect to an (even expectably small) extent of the pozzolanic reaction in the UHPC system, further studies should investigate the strength development at early and late states of hydration in dependence of various silica components, to gain an insight into decisive mechanisms. Especially, the influence of silica characteristics on early hydration should be regarded.

Acknowledgements

The authors thank Johannes Prieschl for the synthesis of the Stoeber particles, Kirsten Langguth and Werner Stracke for their support in taking SEM images and Hans-Jürgen Seel for CSP sample preparation. The research was funded by the Elite Network of Bavaria in the International Graduate School 'Structure, Reactivity and Properties of Oxide Materials' as well as by the German Federal Ministry of Education and Research in the project 'Chemically Bonded Ceramics by Nanotechnological Improvements of Structure (03X0067E)'.

References

[1] Fehling E, Schmidt M, Teichmann T. Entwicklung, Dauerhaftigkeit und Berechnung Ultrahochfester Betone (UHPC) Forschungsbericht DFG FE 497/1-1. Kassel: Kassel University Press; 2005.
[2] Naaman AE, Wille K. The path to ultra-high performance fiber reinforced concrete (UHP-FRC): five decades of progress. In: Schmidt M, Fehling E, Glotzbach C, editors. Proceedings of Hipermat 3rd international symposium on UHPC and nanotechnology for high performance construction materials. Kassel: Kassel University Press; 2012. p. 3–16.
[3] Geisenhanslueke C. Modellierung und Berechnung hochdichter Feinstkornpackungen für Beton. Beton Stahlbetonbau 2005;100(2):65–8.
[4] Schmidt M, Bunje K, Dehn F, Droll K. Sachstandsbericht Ultrahochfester Beton. Berlin: Beuth; 2008.
[5] Schmidt M, Stephan D, Krelaus R, Geisenhanslueke C. The promising dimension in building and construction: nanoparticles, nanoscopic structures and interface phenomena, part 2. Cem Int 2007;5(4):3–11.
[6] Schmidt M. Nanotechnologie: Neue Ansätze für die Entwicklung von Hochleistungsbindemitteln und – betonen. In: Stark J, editor. Proceedings of Ibausil 17th international conference on building materials. Weimar: Finger-Institute for Building Materials; 2009.
[7] Diamond S, Sahu S. Densified silica fume: particle sizes and dispersion in concrete. Mater Struct 2006;39:849–59.
[8] Stoeber W, Fink A. Controlled growth of monodisperse silica spheres in the micron size range. J Colloid Interface Sci 1968;26:62–9.
[9] Masters K. Spray drying handbook. 4th ed. Harlow Essex: Longman Group UK Limited; 1985.
[10] Froehlich S, Schmidt M. Influences on repeatability and reproducibility of testing methods for fresh UHPC. In: Schmidt M, Fehling E, Glotzbach C, editors. Proceedings of Hipermat 3rd international symposium on UHPC and nanotechnology for high performance construction materials. Kassel: Kassel University Press; 2012. p. 225–32.
[11] Shibata M. Cross section specimen preparation device using argon ion beam for SEM. JEOL News 2004;39(1).
[12] Diamond S. Mercury porosimetry An inappropriate method for the measurement of pore size distributions in cement-based materials. Cem Concr Res 2000;30:1517–25.
[13] Schwanda F. Der Hohlraumgehalt von Korngemischen. Beton 1959;9(1):12–7.
[14] Reschke T. Der Einfluss der Granulometrie der Feinstoffe auf die Gefuegeentwicklung und die Festigkeit von Beton Doctoral Thesis. Weimar, Bauhaus University Weimar; 2001.
[15] Reschke T, Siebel E, Thielen G. Influence of the granulometry and reactivity of cement and additions on the development of the strength and microstructure of mortar and concrete (Part 1). Beton 1999;12:719–24.
[16] Tobón JI, Restrepo OJ, Payá J. Comparative analysis of performance of portland cement blended with nanosilica and silica fume. Dynamic 2010;77(163):37–46.
[17] Diamond S, Sahu S, Thaulow N. Reaction products of densified silica fume agglomerates in concrete. Cem Concr Res 2004;34:1625–32.
[18] Pfeifer C, Moeser B, Stark J. Hydratation, Phasen – und Gefügeentwicklung von Ultrahochfestem Beton. In: Stark J, editor. Proceedings of Ibausil 17th international conference on building materials. Weimar: Finger-Institute for Building Materials; 2009.
[19] Qing Y, Zenan Z, Deyu K. Influence of nano-SiO_2 addition on properties of hardened cement paste as compared with silica fume. Constr Build Mater 2007;21:439–545.
[20] Lawner Weinberg S, Knapp Abramowitz S. Data Analysis for the behavioral sciences using SPSS. New York: Cambridge University Press; 2002.
[21] Marchuk V. Dispersibility of the Silica fume slurry in cement paste and mortar. Beton 2002;52(7–8):393–8.